The Bioscan AN INTERNATIONAL QUARTERLY JOURNAL OF LIFE SCIENCES 21(3): 529-548, 2026 www.thebioscan.co

Deciphering Six Decades of Shoreline Evolution along the Open Mahanadi Coast, India: A Compartment-Based Approach

Rajan Boopathy[1,], Yoganandan Veeran [1*], Roop Singh Kankara[2],

1.Department of Marine Science, Bharathidasan University, Tiruchirappalli – 620 024, India

2.National Centre for Coastal Research, MoES-ESSO, Chennai- 600100, India

***Corresponding Author: Yoganandan Veeran**

DOI: https://doi.org/10.63001/tbs.2026.v21.i03.pp529-548

KEYWORDS

Shoreline change, Geomorphic compartments, Long-term Morphological evolution; Net Shoreline Movement (NSM); Linear Regression Rate (LRR); Remote sensing; GIS; Mahanadi Delta.

Received on: 30-06-2026
Accepted on: 25-07-2026
Published on: 31-07-2026

Abstract

Erosion and accretion processes play a significant role in affecting the coastal segment. Before exploring the reasons behind the changes, addressing them spatially along the coast is most important. Only a few studies focused on the coastal changes at the compartment level. Following this, the study aims to analyse long-term decadal changes using a high-resolution dataset to capture spatio-temporal details of the shoreline and morphological evolution within and across compartments. using geospatial techniques with statistical analysis, such as linear regression, to find the long-term trend and net shoreline movement to determine whether the trend is consistent or fluctuating. Areal measurements were estimated to address the morphological evolution over the period. The key results highlight the formation of a wide beach on the southern side of the Paradip port in compartment 1 and the formation of new islands in compartment 7. In contrast, there is a permanent loss of Jagathsingpur Spit at compartment 2, and a complete loss of Hukitola Island at compartment 3 (Hukitola Bay). Specifically, high erosion was noticed at the Pentha stretch (compartment 5), which has impacted the settlements at Satabhaya, a mass nesting site and eco-tourism destination. The compartment-based findings using high resolution and long-term data sets help understand long-term shoreline behavioural patterns and morphological evolution in a detail scale within and across compartments, which will be useful for shoreline mitigation and management

1. Introduction

The Morphodynamic nature of the global shoreline is driven by fluvial, avolien, and marine processes. In a variety of coastal environments, including sandy beaches (Masselink et al., 2006), coral atolls (Barry et al., 2007) tight feedback loops between morphology and hydrodynamic processes result in dynamic landscapes. Long and short-term shoreline changes are caused by a range of natural and anthropogenic processes along the coast (Albert and Jorge, 1998; Murali et al., 2015). In particular, these dynamic shorelines are widely shaped by a range of natural processes, including waves, tides, currents, and longshore transport. Along with these extreme events, such as storm surge and tsunamis, play a significant role in the drastic change in shoreline morphology. In addition, during high-energy nearshore dynamic conditions, anthropogenic effects threaten shorelines and cause coastal flooding and erosion. Recent studies found a drastic concentration of the global coastal population within a 10km stretch. Such coastal areas exhibit various morphological features, and their ecosystems serve as habitats for various creatures; among these, human pressure is a dominant factor. According to a recent NASA study, 31% of the global shoreline is sandy shore. Among them 24% are eroding at the rate of 0.5m per year NASA. (2025). Recent research shows that 34% of the Indian coast is eroding (Kankara et al., 2018). Many researchers have studied both long and short-term shoreline changes along the east coast of India. Along the Indian coast, one of the most predominant erosion sites was reported in Odisha. (Murali et al., 2009) monitored the shoreline of the Paradip stretch using Landsat imagery from 1973 to 2005 and observed significant morphological changes, including a loss of beach area and shoreline realignment. (Mohanty et al., 2015) studied shoreline changes near ports along the Odisha coast using field observations and satellite imagery and observed accretion on the southern side of the ports and erosion on the northern side. (Markose et al., 2016) studied shoreline changes using multi-temporal satellite imagery from 1990 to 2014 along the Ganjam coast and found that frequent cyclones and anthropogenic impacts play a significant role in shoreline changes. (Roy et al., 2018) examined shoreline changes using Landsat imagery from 1990 to 2015 and found that 46% of the Odisha coast was under erosion, 36% was accreting, and 18% was stable. (Manoranjan Mishra et al., 2019) investigated and analyzed long- and short-term shoreline changes using Landsat imagery and documented hotspots along the southern coast of Odisha. (Kar et al., 2021; Pradhan et al., 2024) have observed accelerated shoreline erosion along the Mahanadi delta front and emphasized that the Pentha stretch was drastically eroding in Odisha. From previous studies conducted across different temporal and spatial regions of Odisha, a commonality among all was the use of Landsat datasets. And also, instead of viewing the coast as a single continuous line, it should be divided into compartments. In geomorphology, connectivity science is a growing field of study that examines how components of complex systems relate to one another. Compartment-based long-term shoreline behaviour and morphological evolution are essential for understanding overall coastal change over time. It is dominated by sandy shores with various geomorphic features, including spits, ridges, dunes, and beach morphology, as well as islands. These fronts also host mangrove ecosystems, Bhitarkanika National Park, Gahirmatha Marine Sanctuary, a mass nesting ground, and support many economic activities such as Eco-tourism and port activities. In such a significant site, only a few addressed the local erosion and accretion trends. In light of this, the study aims to quantify long-term shoreline changes and morphological evolution within and across the compartments using predominantly decadal fine-resolution satellite images to understand long-term erosion and accretion patterns, consistent or fluctuating trends, and areal morphological evolution. Such studies will be useful for coastal managers, geomorphological researchers, and scientists for understanding compartment-based morphological and shoreline behaviour within and across the coastal system.

2. Study area

The study area lies in the northern part of Jagathsingpur Kendrapara and in the southern part of Balasore district, Odisha state, India, specifically between the coordinates of 20. 2013 latitude and 86.558 Longitude at the southern boundary, and 20.827 latitude and 86.982 longitude at the northern end. Along the study area, the shoreline extends 162km and is discontinuous due to natural features such as river mouths and bathymetry, as well as artificial structures such as breakwaters. To quantify the local changes within each segment, the study area was divided into 7 compartments.

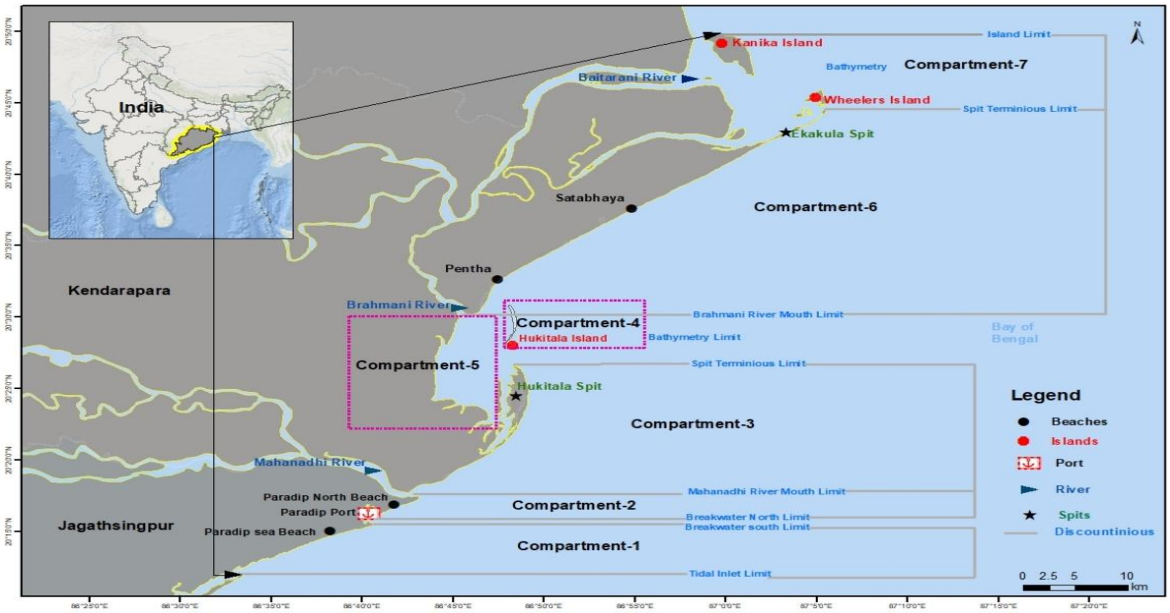

Figure 1- Map showing the study, divided into 7 compartments.

2.1 . Compartment 1

Compartment 1 covers a distance of 8.96km and has a sandy beach, where it is bounded by the mouth of the distributary channel at the southern side and the southern breakwater of Paradip port at the northern side. Paradip port was a natural deep-water port and one of the oldest ports in India, located at the Mahanadi delta. National and international trade play a significant role in a state's and a country's economy. At the southern side of the port was one of India's longest beaches, dominated by tourism activity. The existing compartment houses trade and tourism, thereby enhancing its economic significance.

2.2 . Compartment 2

Compartment 2 covers a distance of 6 km laid with the armoured structure. The segmented coast is limited by the Port's northern breakwater on the southern side and the Mahanadi river mouth on the northern side of the compartment.

2.3 . Compartment 3

Compartment 3 covers a distance of 19.72 km and features a spit on the southern side, bounded by the Mahanadi river mouth and open-sea bathymetry at its southern end. And it encompasses the ridges and sandy beaches.

2.4 . Compartment 4 and 5

Compartment 4 covered a distance of 9.96 km, an island segment located at the Hukitola bay. And compartment 5 is a shadow coast covering 23.75 km, dominated by the mangrove ecosystem. And hence the compartment preserves the high ecological value.

2.5 . Compartmemt 6

Compartment 6 covers a distance of 41.62km, dominated by the sandy coast, which features ridges on the southern side, isolated dunes on the backshore, and a spit on the northern side. The segment is bounded by the Brahmani River at the southern end and by open bathymetry at the north spit terminal end. Pentha is a prominent eroding site, located a few km from the river mouth. And gabions were installed for the short distance as an erosion mitigation measure. Between the Brahmani river mouth and Pentha, seasonal recreational activities were centered. Bhitarkanika National Park was located at the back barrier zone, a few kilometers north of Pentha. And parallel to it, along the coast, is the turtle nesting site.

2.6 . Compartment 7

Compartment 7 was an Island vicinity. Wheeler Island, also called Dr. Abdul Kalam Island, is located on the southern side and covers a distance of 8.7km. And it was dominated by the sandy coast at the south east, north east, and south west, which is stabilized by the armoured structures. Similarly, in the north, Kannika Island is sheltered by the mangroves and spans 17km. Overall, the study area shows that the compartments are ecologically, geomorphologically, and economically significant sites.

3. Materials and methodology

Satellite images of varying scale and field surveys have been used to emphasize the coastal morphological evolution with shoreline position trend at short (< 10 years) and medium-term scales (between 10- and 60-years) (Crowell et al., 1993). The interpretation period (1965-2024) covers 54 years. For the investigation of beach behaviour, multi-date satellite photos of corona, Landsat TM, and ETM+ IRS images were employed in the following table 1.

Satellite	Sensor	Date of image acquisition	Resolution (m)	Data source
Corona	KH-4A	05-28-1965	2.74	USGS
Landsat	MSS	01-17-1973	57	USGS
Corona	KH-9	04-04-1978	6.09	USGS
Landsat	TM	11-29-1990	30	USGS
Landsat	ETM	10-23-2000	30	USGS
Cartosat	Pan	07-07-2006	2.5	NRSA
IRS-P6	LISS-IV	10-21-2012	5.8	NRSA
IRS-P6	LISS-IV	03-14-2013	5.8	NRSA
IRS-P6	LISS-IV	05-20-2014	5.8	NRSA
IRS-P6	LISS-IV	04-21-2015	5.8	NRSA
IRS-P6	LISS-IV	03-22-2016	5.8	NRSA
IRS-P6	LISS-IV	03-17-2017	5.8	NRSA
IRS-P6	LISS-IV	10-23-2018	5.8	NRSA

IRS-P6	LISS-IV	02-11-2019	5.8	NRSA
IRS-P6	LISS-IV	10-21-2021	5.8	NRSA
IRS-P6	LISS-IV	04-08-2024	5.8	NRSA

Table 1 showing the Multi-temporal satellite images from 1965 to 2024

Ground control points were acquired utilizing a handheld Trimble geo-explorer 6000 series global positioning system to minimize the rectification error and maintain positional accuracy for the satellite images. To acquire GCPs, the device employed WGS 1984 projection with a minimal inaccuracy of 2m. Permanent characteristics such as building corners and road intersections were used in the selection of GCPs **(Fig-3)**. A polynomial second order transformation in Erdas Imagine 2013 software was used to rectify the base image utilizing GCPs collected in the field. Between 15 to 25 points of GCPs were randomly placed in the satellite Image. Other set of temporal images were also corrected utilizing the master image by image-to-image co-registration method. In Erdas platform all images are converted into UTM (45 North Zone) projection for shoreline extraction. The following equation of root mean square error (RMSE) approach was used to calculate and check the accuracy of georeferenced images. Minimum of 6 to 7 field points were used for each image in order to calculate the RMSE. The RMSE was maintained to less than 1 pixel for LISS – 1V, Cartosat, Corona images, and 25m for Landsat images (Markose et al., 2016).

$$RMSE = \sqrt{\sum_{i=1}^{n}[(x_s - x_r) + (y_s - y_r)^2]^2}$$

Where x_s and y_s are the spatial coordinates of GCPs and x_r and y_r are the spatial coordinates of the same point on a rectified satellite image Markose et al. 2016.

3.1 Shoreline detection and extraction.

The spatiotemporal position of historical shorelines determines the coast's morphological evolution. There are different proxies were used for monitoring the historical shoreline variations e.g, vegetation line (Hoeke et al., 2001), dune line (Stafford and Langfelder, 1971), bluff top/cliff top (Guy Jr, 1999; Priest, 1999), high water line (Dolan et al., 1980; Fenster and Dolan, 1999; McCurdy, 1950;

Shalowitz, 1964; Zhang et al., 2002). For historical shoreline comparison studies, (Crowell et al., 1991) determined that high water lines were the most reliable indicators, which are plainly visible in both field and aerial images (Stafford and Langfelder, 1971) High water line was a consistent proxy for shoreline detection among the various methods. As part of this investigation, the satellite images were manually processed to determine the wet/dry line of the last high tide. The error associated with tidal range can be reduced by using wet/dry line as a shoreline proxy (Kankara et al., 2015, 2014).

3.2 Trend analysis across compartments

Historical shoreline changes and spatial morphological variances were used to identify a coastal trend. Digital shoreline analysis system (DSAS) in GIS environment was used to undertake shoreline change study to identify trends. As a result of the statistical approach of linear regression, net shoreline movement, transects were generated at 20 m intervals to calculate the shoreline change. By fitting the best fit line linear regression quantify the shoreline changes using all shoreline positions (Crowell et al., 1991). It is calculated as

$$\boldsymbol{m} = \frac{\boldsymbol{n}\sum \boldsymbol{xy} - \sum \boldsymbol{x} \sum \boldsymbol{y}}{\boldsymbol{n}\sum \boldsymbol{x}^2 - (\sum \boldsymbol{x})^2}$$

Where m is the slope which address the shoreline change meters per year.Linear regression helps to understand the long-term erosion and accretion trend within and across the compartment. Net shoreline movement helps to understand the displacement of shoreline between oldest and the recent position

$$\boldsymbol{NSM} = \mathbf{Distance}_{\mathbf{latest\ shoreline}} - \mathbf{Distance}_{\mathbf{earliest\ shoreline}}$$

Where D represents the cross-shore distance from the baseline.

Net shoreline movement helps to understand the consistent erosion, accretion and fluctuating coast. Net shoreline movement were applied more specifically for the eroding coast and for understanding the temporal influences, before and after events. Areal measurements were applied for morphological features, includes spits, island for understanding the evolution over time. Linear regression using slope of the line helps to understand the long-term temporal shoreline changes. And net shoreline movement shoreline movement (NSM) measures the distance between each transect's oldest and youngest coastline. Using satellite images Areal measurements in square kilometres helps to understand the morphological changes. In a compartment where erosion accretion trends are the same, the environment has been following the same trend for a long period of time (past55 years). Accretion is shown by positive values, erosion by negative values, and no change is indicated by zero. stability. The long-term analysis, consistent trend analysis, and areal measurement shows how strong the pattern of erosion and accretion trend influences the coastal environment with respect to time.

4. Results

To quantify the long and short-term (specifically event-based) shoreline changes within and across the compartments, the study was divided the continuous coastal segment into 7 compartments with overall map along with results **(Fig 2)** and table **(Table 2)** shown in the below.

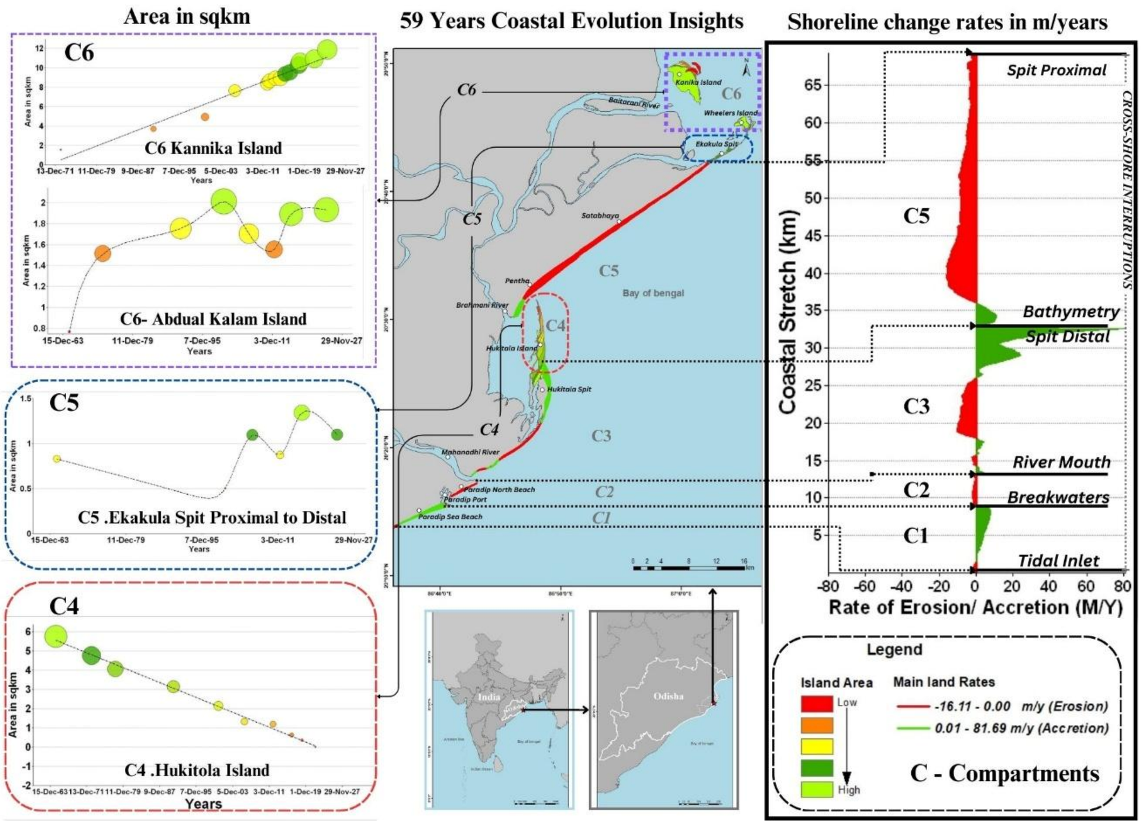

Figure 2 Map along with graphs showing compartment wise results over the period of 59 years

Compartments	Geomorphic Type	Shoreline Length	Boundaries	Erosion/Accretion length	Longterm - Trend: Rate of Change Lrr in (m/yr)	Short term: Important Events	Short term: NSM in m	Area: in sqkm	Status
C1	Main Land (Paradip Sea Beach)	8.96 km	Southern limit tidal inlet	1.54	-1.14	1965 to 1973	-1.98		Fluctuation
						1965 to 2000	-74.62		
						1965 to 2012	19.69		
						1965 to 2024	-74.28		
			Northern limit (southeren Breakwater)	7.42	6.18	1965 to 2024	389.63		Accretion
C2	Main Land (Nehru Bangala)	5	Southern limit (northeren Breakwater)	5	-1.37	1965 to 1973	-89.53		Erosion
			Northeren limit (Mahanadhi River Mouth)			1965 to 1978	-136.89		
						1978 to 2024	15.41		Fluctuation
	Spit 1 (Jagathsingpur Spit)	13.2	Conflunce of mahanadhi river mouth Spit terminious	13.2	0.1	1965		1.71	Accretion
						1973		2.94	
						1978		3.77	
						1980		4.16	Erosion
						1990-2024		0	No Spit (After 1990)
C3	Spit 2 (Hukitola Spit)	19.72	Southern limit (Mahanadhi River Mouth)	12.96	-4.09	1965		1.01	Fluctuation
						1973		1.73	
						1978		2.65	
						1990		6.15	
						2000		6.55	
						2006		7.16	
			Northeren limit (Spit Distal Point)	6.76	19.7	2012		10.83	Accretion
						2016		10.82	
						2019		11.58	Stable
						2024		11.58	
C4	Island (Hukitola Island)	9.96	Open sea bathymetry (Northeren Island)	9.96	0.1	1965		5.74	Countiniously Eroding
						1973		4.73	
						1978		4.04	
						1990		3.13	
						2000		2.12	
						2006		1.31	
						2012		1.17	
						2016		0.6	
						2019		0.34	
						2022		0.1	Completely Eroded in 2022
C5	Main land (Mahanadi Delta Mangroves)	23.75	Shadow coast	23.75	412.75	1965-2024	-		Countiniously Accreting
C6	Main Land (Pentha Stretch)	37.8	Southern limit Brahmani River Mouth	3.1	7.16	1965 to 1973	-103.6		Erosion
						1965 to 1978	18.1		Accretion
						1965 to 1990	97.32		
						1965 to 2000	206.53		
						1965 to 2016	319.81		
						2016 to 1990	6.92		Erosion
			Northern limit (Spit proximal portion)	34.7	-7.81	1965 to 2024	-477.82		Countinious Erosion
C7	Spit 3 (Ekakula Spit)	7.7	Southern limit (Spit Proximal Portion)	-	-	1965		0.82	Fluctuation
						1973		0.53	
						1990		0.46	
			Northern limit (Spit distal Portion)			2000		0.5	
						2012		0.87	
						2016		1.34	
						2024		1.09	
	Island 1 (Dr. Kalam Island)	8.7	-	-	-	1965		0.76	Fluctuation
						1973		1.51	
						1990		1.75	
						2000		2	
						2012		1.55	
						2016		1.89	
						2024		1.93	
	Island 2 (Kanika Island)	17	-	-	-	1973		1.5	Countinious Accretion
						1990		3.68	
						2000		4.92	
						2012		8.36	
						2016		9.35	
						2024		11.85	

Table 2 show the compartment wise shoreline and the morphological changes over the period of 59 years

5.1 Compartment 1

It is bounded between the distributary channel at the south and the Port's southern breakwater at the north. On the southern side, specifically along the coast 1.54km from the channel, measured regression analysis indicates an erosion trend of 1.14m over 59 years. In each cumulative trend for the southern side, the net shoreline movement reveals erosion and accretion of

-1.98m, -74.62m, 19.69m, and again -74.28m for the following corresponding periods between 1965 and 1973, 1965 and 2000, 1965 and 2012, and 1965 and 2024. On the northern side, from the southern breakwater, 7.4km towards the south shows an accretion trend. The long-term regression trend shows 6.18m/year. Since the northern beach shows an accretionary trend, the cumulative trend was focused only on the net shoreline movement between 1965 and 2024. Overall, the net shoreline movement indicates that a wide beach measuring 389.63 meters was formed between 1965 and 2024.

5.2 Compartment 2

It is bounded by the northern breakwater to the south and the river mouth to the north. The long-term analysis from 1965 to 2024 shows a linear regression erosion slope of 1.37m per year. This was cross-checked with different periods of cumulative analysis using the net shoreline movement. And it shows that the net shoreline movement was -89.52m, -136.89m in the following period between 1965 and 1973, 1965 and 1978. But from 1978 TO 2024, the net shoreline movement results show the accreting trend of 15.41m **(Fig-2 and Table 2).**

Before 1980, a 13.2 km-long spit was documented attached at the northern end. In 1965, 1973, 1978, and 1980,the spit's area was 1.71 sq km, 2.94 sq km, 3.77 sq km, and 4.16 sq km, respectively. And after 1980 till 2024, no spit formation was recorded **Fig-3**.

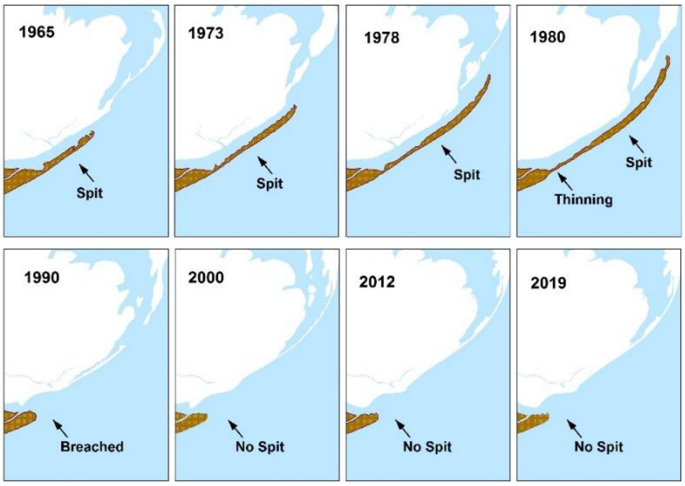

Figure 3 Map shows Evolution and Paramanent loss of spit after 1980

5.3 Compartment 3

Compartment 3 was bounded between the river mouth at the south and the open bathymetry at the spit terminal. The result of long-term regression analysis shows erosion at a rate of 4.90m/year on the southern side **(Fig-2 and Table 2)**. Whereas on the northern side of the spit, the results show a high rate of accretion ,19.7 meters per year. The areal result shows that, initially in 1965, the area was 1.01 sqkm and gradually increased to 1.73 sq km in 1973 and 2.65 sq km in 1978. But in 1990, 2000, and 2006, the areal results show rapid growth of 6.15 sq km, 6.55 sq km, and 7.16 sq km. From 2012, 2016, 2019, and 2024, the results show 10.83 sq km, 10.82 sq km, 11.58 sq km, and 11.58 sq km, respectively **Fig-4**.

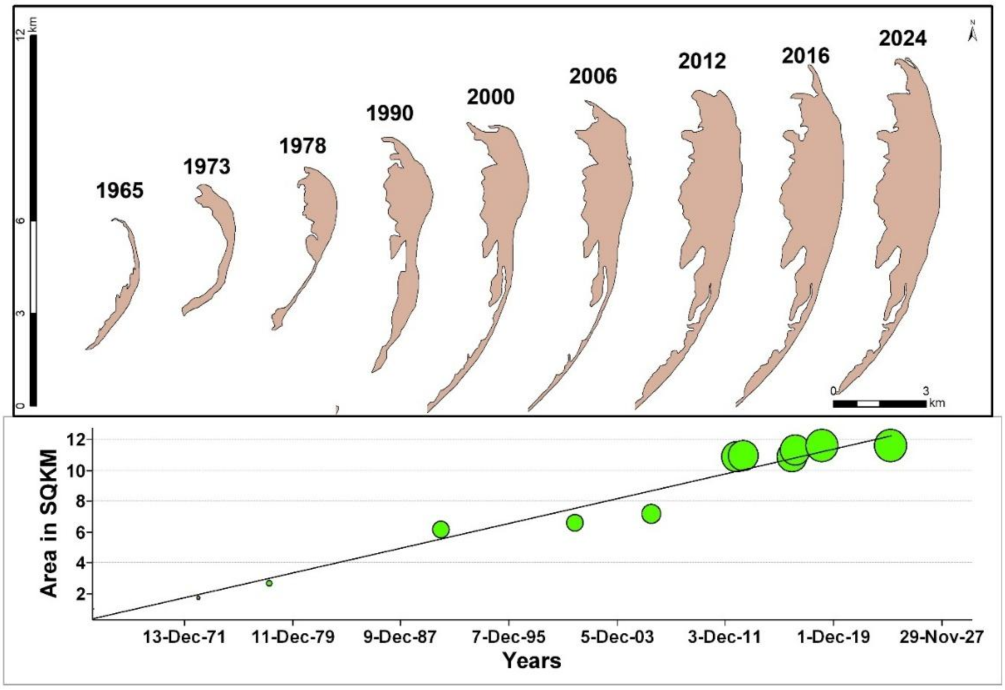

Figure 4 Map show evolution of Hukitola spit (compartment 3)

5.4 Compartment 4

Compartment 4 was an Island segment. The areal extent of the Island in 1965, 1973, and 1978 was 5.74 sq km, 4.73 sq km, and 4.04 sq km, respectively. But in 1990, 2000, and 2026, the areal extent was rapidly reduced to 3.13 sq km, 2.12 sq km, and 1.31 sq km, respectively. Furthermore, in 2016 and 2019, the Island's area was severely eroded to 0.6 and 0.34 sq km. The Island migrated up to 4.5km towards the north and fully submerged and eroded at Hukitola Bay on the 5th of November 2021 **Fig-5 & 6**.

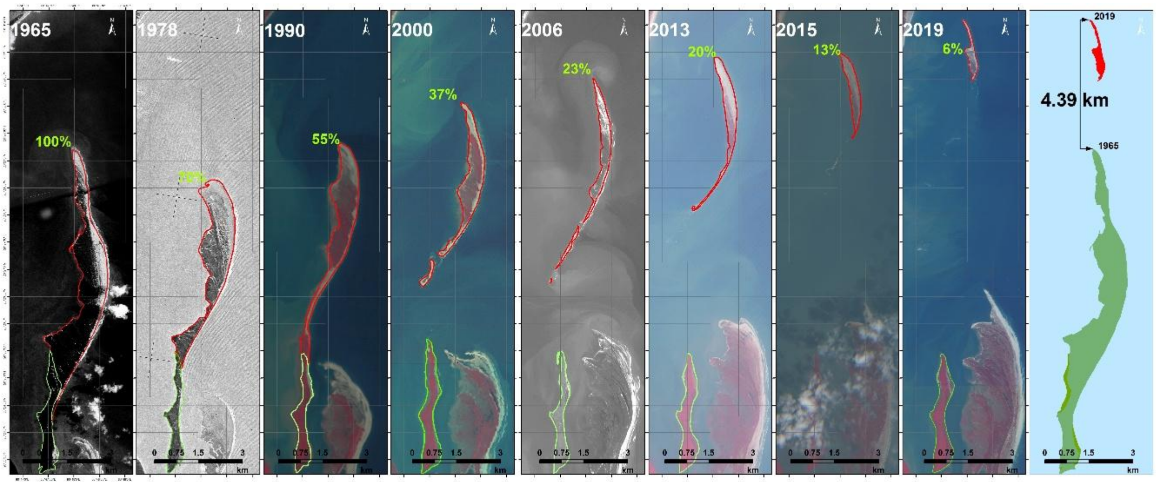

Figure 5 Map show shrinking and migration of island at compartment 4

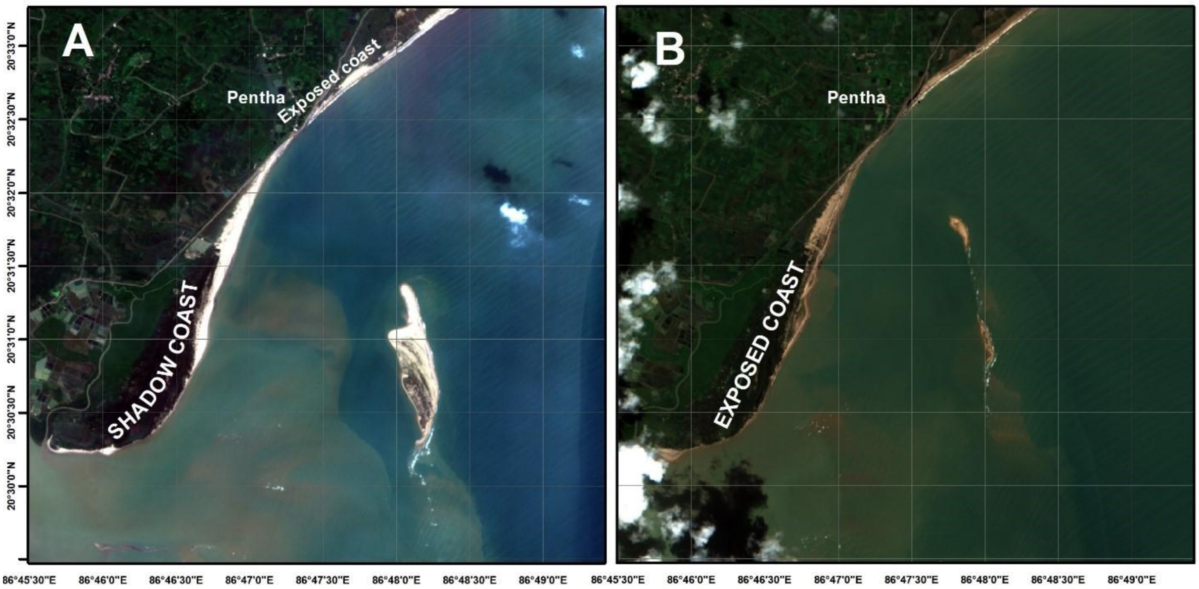

Figure 6 satellite image shows eroded island. A. show the sentinel image acquired on 2018 and B. show the island eroded in sentinel image acquired on 5th of November 2021.

5.5 Compartment 5.

Compartment 5 was a sandy coast and mangrove ecosystem, located behind Compartment 3, a spit feature. Linear regression shows that the coast was accreting at the rate of 23.7 meters per year. And the net shoreline movement between 1965 and 2024 also shows the accreting trend of 412.75 meters **(Fig-2 and Table 2).**

5.6 Compartment 6.

Compartment 6 was bounded by the mouth of the Brahmani River to the south and by open bathymetry to the north. Bathrakannika National Park is located behind the backshore of the north-west, a turtle mass-nesting site along the coast, specifically in the north. And tourism activity is carried out on the southern side.

1. **River mouth (southern limit) till Pentha**

Along the coast from the southern limit to the north of Pentha, long-term linear regression analysis shows that the southern coast accreted at the rate of 7.16 meters per year. The net shoreline movement between 1965 and 1973 shows the erosion trend of 103.6 meters. And the trend turned to an accreting phase during the net shoreline movement analysis of 1965 and 1978, with a rate of 18.1 meters. And the trend was continuous for the subsequent net shoreline movement analysis between 1965 and 1990, 1965 and 2000, and 1965 and 2016 at rates of 97.32m, 206.53m, and 319.81m, respectively **(Fig-2 and Table 2).** But the trend was reversed during the net shoreline movement analysis between 2016 and 2022, which shows an erosion rate of -6.92 meters **Fig-7**.

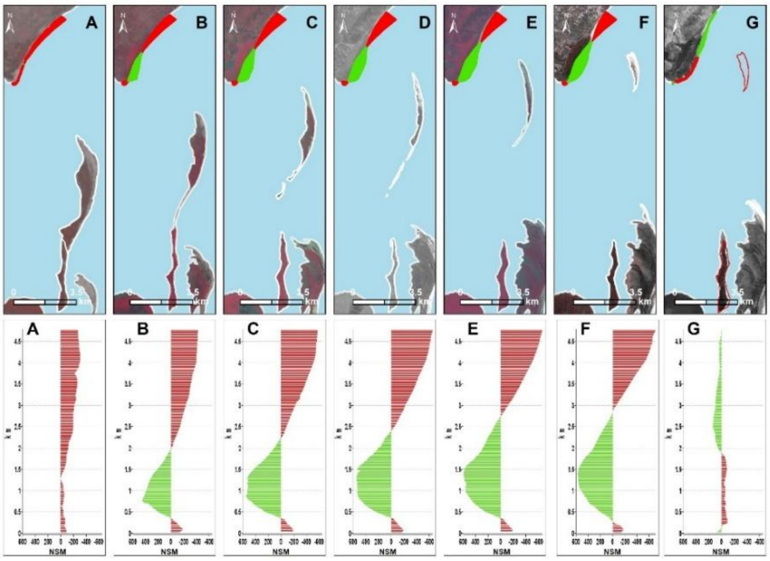

Figure 7 southern stretch transforming from accreting to eroding coast. A-1965-1973, B-1965-1978, C-1965-1990, D--1965-2000, F-1965-2016, G-1965-2016

2. **Pentha to Ekakula Spit**

The last 59 years' results of linear analysis for the long-term show that the coast was under an erosion trend at the rate of 7.81 meters per year. Along the coast, results from net shoreline movement also show the erosion trend of -477.82 meters between 1965 and 2024 **(Fig-2 and Table 2)**. And specifically, at Pentha, between 1965 and 2024, the net shoreline movement was towards land at the rate of 900 meters **Fig-8**.

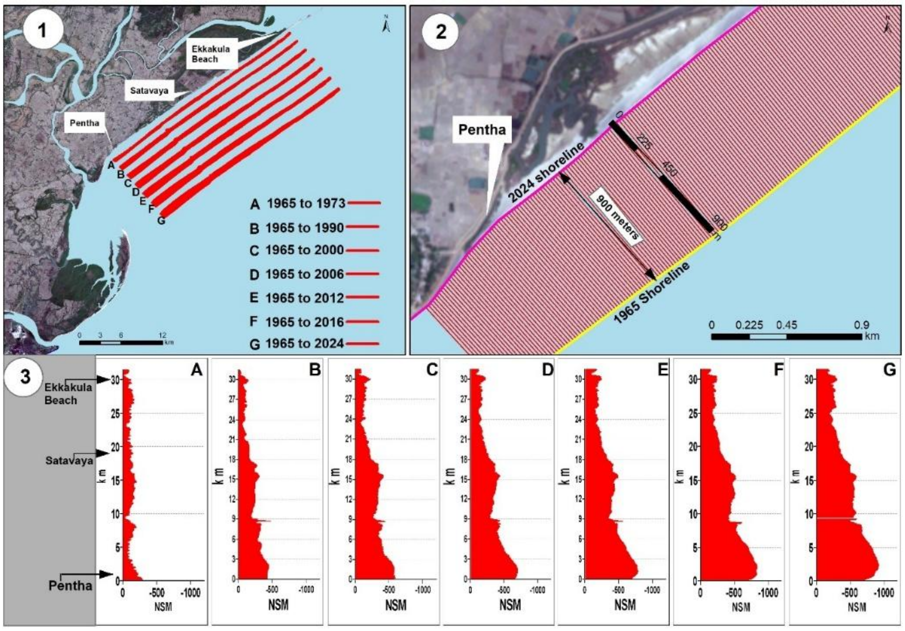

Figure 8: Map(1) and graph (3) show continuous erosion along the compartment 6 from Pentha to Ekakula spit. Map (2) shows the drastic erosion at Pentha

5.7 Compartment 7

It was an Island coast. The multi-temporal satellite images show the areal evolution measurements of Wheelers and Kannika Island. During the aerial measurements of Wheelers Island in 1965, the area was 0.76 sq km. And in 1973, 1990, and 2000, the area increased rapidly to 1.51 sq km, 1.75 sq km, and 2 sq km. Again, the areal extent was reduced to 1.55 sq km in 2012. However, during the area measurements in 2016 and 2024, the area increased to 1.89 sq km and 1.93 sq km, respectively **(Fig-2 and Table 2) & (Fig-9A).** Whereas for Kannika Island, the area extent was 1.5 sq km in 1965. And it was rapidly increased to 3.68 sq km, 4.92 sq km, 8.36 sq km, 9.35 sq km, and 11.85 sq km in the subsequent years of 1990, 2000, 2012, 2016, and 2024 **(Fig-9 B).**

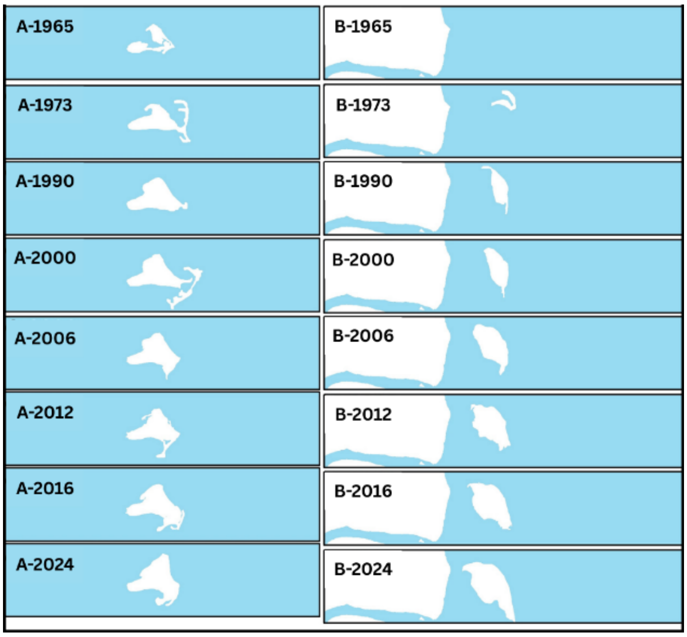

Figure 9 Map (A) shows the evolution of Wheelers (Dr.Abdul Kalam) Island and Map (B) shows the evolution of Kannika Island from embryo

5. Discussion

The long-term analysis, consistent trend analysis, and areal measurement help understand behavioral performance within and across the compartments. This shows continuous erosion, accretion, or fluctuation in the erosion and accretion trends across the compartments.

5.1 Dominated Trend within the compartment

Beginning from the south, compartment 1 results show a fluctuating erosion-accretion trend at the southern side and continuous accretion at the northern side. And the majority of the compartment was accretion-dominated. This was supported by the (Mohanty et al., 2015) have documented that perpendicular structures results in accretion at the southern side of the Paradip port. In Compartment 2, the area was fully covered by the armoured coastal structures, indicating that the coast was previously eroding and the structures were installed to prevent further erosion. This shows that negative consequence at the northern port due to the impacted shore of shoreline perpendicular structure (Mohanty et al., 2015). Compartment 3 was an accreting zone. A spit segment that continuously extended northward between 1965 and 2024. However, it is influenced by both erosion and accretion factors in the south. Compartment 4 was an erosion-dominated zone. Shrinking Island was continuously undergoing erosion and finally retreated in November 2021. Compartment 5 results indicate the accreting zone, which is barriered by the spit features of compartment 3. Compartment 6 was dominated by erosion (Kar et al., 2021; Mishra et al., 2023; Pradhan et al., 2024) . However, a stretch of accreting zone, including ridges at the southern boundary and a dynamic spit at the northern end, was also incorporated into the highly eroding site. Results from compartment 7 show that the segment was an actively accreting zone; however, the fluctuations in erosion and accretion were seen on Wheelers Island, whereas on Kannika Island, on the northern side, continuous accretion was observed. These results help to understand and describe the dominant controlling factor, such as erosion, accretion, or fluctuation trend, acting within the compartment over the past 59 years.

5.2 Behaviour Pattern and evolution over time.

Results demonstrate the long-term, consistent trend, and the areal measurements are the shoreline morphological response to the corresponding marine process. It clearly shows that the southern side of compartment 1 was eroding and the northern side was continuously accreting. Following this, the result for compartment 2 shows that until 1978 erosion was dominant, but from 1978 to 2024 it shows a stable-to-low accreting pattern. The result also highlighted that the coast was welded with the spit features. The dominant spit features were visible until 1980, after which they were completely eroded. There was no evidence of spit formation until 2024. In compartment 3, over time, the amount of spit developed gradually until 1978, and it rapidly increased after 1978. And its accelerated growth was observed towards the north. However, the long-term analysis shows erosion on the southern side and continuous accretion at the northern side of the spit. Whereas compartment 4 was an Island segment, aerial measurements of long-term results reveal a gradual shrinkage, migration, and complete erosion in November 2021. Compartment 5 was a mangrove ecosystem, and the results emphasize that the coast was accreting from 1965 to 2024. Moreover, compartment 6 was a tricky coast, where both accreting and eroding beaches were noticed during the analysed period. At the southern end of the compartment, from the river mouth to the southern side of the Pentha, the results show an accreting trend till 2016. But after 2016, the trend was reversed to an eroding phase, and it continued until 2024. And further from Pentha to the Ekakula spit, the results show continuous erosion. More specifically, at the Pentha show, erosion is of greater magnitude compared to other places within the compartment. Finally, the results of compartment 7 show the active accreting zone.

Long-term results clearly indicate that erosion or fluctuation patterns were observed on the southern side and accretion on the northern side, specifically within the compartment. This evidence can be noticed within all compartments. Whereas across the compartment, the northern side of the southern compartment shows accretion, and the southern side of the northern compartment shows erosion. And this evidence is observed between compartments 1 and 2, where the southern side of the Paradip port was accreting, and the northern side was eroding. Similarly, between compartments 3 and 4, in which compartment 3 was a spit feature that showed continuous accretion, and northern compartment 4 was an Island feature that was continuously eroding. Compartment 5 was in a shadow region, which is barriered by the spit feature of compartment 3. A similar trend was observed between compartments 3 and 6: compartment 3 was an accreting spit feature, and compartment 6 was a sandy coast that was continuously eroding and accumulated in compartment 7. Along with this patterns, detailed captured morphological evolutions over time within and across the compartments such as permanent loss of spit features at compartment 2, migration and complete loss of Hukitola Island in compartment 4 and recently started to eroding at south of Pentha (compartment 6), and the eroded materials are forming as new islands at the north (compartment 7) all shows the significance of compartment-based analysis for the long period using high resolution data sets.

6. Conclusion

Last 6 decadal results show the evident of documented shoreline and the morphological evolution occurred within and across the compartments. In 1965 after the construction of Paradip port, a wide beach was formed at the southern side of the port. Despite this, the beach at the northern side of the port was eroded. However, the coast was stabilized using armoured structures and the erosion was arrested before 1978. But prominent spit features which was noticed till 1980 was completely eroded and its formation was completely prohibited. This conclude that the permanent loss of spit features which was at the edge of compartment 2. And subsequently in compartment 3 a transition of gradual to rapid growth of spit features was noticed from 1990 onwards. These changes between compartment 1,2 and 3 emphasis the impact of structures caused the shoreline and the morphological evolution over the period of last 6 decades. Parallelly during the development of spit in compartment 3, there was a gradual erosion of Island in compartment 4. And finally, the island was completely eroded in November 2021. This shows that the link between the spit development and the island erosion. Compartment 5 consistently developing with the mangrove environment. Compartment 6 play a key role in understanding the complex system, before 1973 southern side of compartment 6 was eroding but after 1973 it started to accreted till 2016. Whereas after 2016 the coast was transformed to eroding segment which influence the active seasonal eco-tourism. And continuous eroding along the compartment 6 with dynamic spit features feeding the emerging islands in compartment 7. Dr Abdul Kalam island show fluctuation in erosion and accretion trend whereas Kannika show the continuous accretion from 1980 onwards. All these evident emphases the significant of the study which show the detail connected morphological evolution, patterns, Persistent and the consistent shoreline changes within and across the compartments in a large scale using long term high resolution multi-temporal satellite datasets. The study overall concludes, compartment-based analysis for the long period using high resolution data sets, if possible, with sub meter data set give the understanding of shoreline and the morphological behaviour with in and across the compartments. Further which helps for the shoreline mitigation and management purpose.

References

3. Albert, P., Jorge, G., 1998. Coastal changes in the Ebro delta: Natural and human factors. J. Coast. Conserv. 4, 17–26.
4. Barry, S.J., Cowell, P.J., Woodroffe, C.D., 2007. A morphodynamic model of reef-island development on atolls. Sediment. Geol. 197, 47–63.
5. Crowell, M., Leatherman, S.P., Buckley, M.K., 1993. Shoreline change rate analysis: long term versus short term data. Shore and Beach 61, 13–20.
6. Crowell, M., Leatherman, S.P., Buckley, M.K., 1991. Historical Shoreline Change: Error Analysis and Mapping Accuracy. J. Coast. Res. 7, 839–852.
7. Dolan, R., Hayden, B.P., May, P., May, S., 1980. The reliability of shoreline change measurements from aerial photographs. Shore and beach 48, 22–29.
8. Fenster, M.S., Dolan, R., 1999. Mapping erosion hazard areas in the city of Virginia Beach. J. Coast. Res. 58–68.
9. Guy Jr, D.E., 1999. Erosion hazard area mapping, Lake county, Ohio. J. Coast. Res. 185–196.
10. Hoeke, R.K., Zarillo, G.A., Synder, M., others, 2001. A GIS based tool for extracting shoreline positions from aerial imagery (BeachTools). US Army Engineer Research and Development Center Vicksburg, MS, USA.

11. Kankara, R.S., Murthy, M.V.R., Rajeevan, M., 2018. National assessment of shoreline changes along Indian coast—A status report for 1990--2016, NCCR Publication.
12. Kankara, R.S., Selvan, S.C., Markose, V.J., Rajan, B., Arockiaraj, S., 2015. Estimation of long and short term shoreline changes along Andhra Pradesh coast using remote sensing and GIS techniques. Procedia Eng. 116, 855–862.
13. Kankara, R.S., Selvan, S.C., Rajan, B., Arockiaraj, S., 2014. An adaptive approach to monitor the Shoreline changes in ICZM framework: A case study of Chennai coast.
14. Kar, P.K., Mohanty, P.K., Pradhan, S., Behera, B., Padhi, S.K., Mishra, P., 2021. Shoreline change along Odisha coast using statistical and geo-spatial techniques. J. Earth Syst. Sci. 130. https://doi.org/10.1007/s12040-021-01703-1
15. Manoranjan Mishra, M.M., Pritam Chand, P.C., Namita Pattnaik, N.P., Kattel, D.B., Panda, G.K., Manmohan Mohanti, M.M., Baruah, U.D., Chandniha, S.K., Subrat Achary, S.A., Tapan Mohanty, T.M., 2019. Response of long-to short-term changes of the Puri coastline of Odisha (India) to natural and anthropogenic factors: a remote sensing and statistical assessment.
16. Markose, V.J., Rajan, B., Kankara, R.S., Chenthamil Selvan, S., Dhanalakshmi, S., 2016. Quantitative analysis of temporal variations on shoreline change pattern along Ganjam district, Odisha, east coast of India. Environ. Earth Sci. 75, 929. https://doi.org/10.1007/s12665-016-5723-1
17. Masselink, G., Kroon, A., Davidson-Arnott, R.G.D., 2006. Morphodynamics of intertidal bars in wave-dominated coastal settings—A review. Geomorphology 73, 33–49.
18. McCurdy, P.G., 1950. Coastal delineation from aerial photographs. Photogramm. Eng. 16, 550–555.
19. Mishra, M., Chand, P., Beja, S.K., Santos, C.A.G., Silva, R.M. da, Ahmed, I., Kamal, A.H.M., 2023. Quantitative assessment of present and the future potential threat of coastal erosion along the Odisha coast using geospatial tools and statistical techniques. Sci. Total Environ. 875. https://doi.org/10.1016/j.scitotenv.2023.162488
20. Mohanty, P.K., Barik, S.K., Kar, P.K., Behera, B., Mishra, P., 2015. Impacts of ports on shoreline change along Odisha coast, in: Procedia Engineering. Elsevier Ltd, pp. 647–654. https://doi.org/10.1016/j.proeng.2015.08.339
21. Murali, R.M., Dhiman, R., Choudhary, R., Seelam, J.K., Ilangovan, D., Vethamony, P., 2015. Decadal shoreline assessment using remote sensing along the central Odisha coast, India. Environ. Earth Sci. 74, 7201–7213. https://doi.org/10.1007/s12665-015-4698-7
22. Murali, R.M., Shrivastava, D., Vethamony, P., 2009. Monitoring shoreline environment of Paradip, east coast of India using remote sensing. Curr. Sci. 79–84.

23. Pradhan, S., Pradhan, U., Samal, R.N., Behera, D., Nanda, S., 2024. Shoreline Changes Along Bhitarkanika Sanctuary, North Odisha Coast, India BT - Geo-Environmental Hazards using AI-enabled Geospatial Techniques and Earth Observation Systems, in: Choudhury, T., Koley, B., Nath, A., Um, J.-S., Patidar, A.K. (Eds.), . Springer Nature Switzerland, Cham, pp. 77–90. https://doi.org/10.1007/978-3-031-53763-9_5
24. Priest, G.R., 1999. Coastal shoreline change study northern and central Lincoln County, Oregon. J. Coast. Res. 140–157.
25. Roy, S., Mahapatra, M., Chakraborty, A., 2018. Shoreline change detection along the coast of Odisha, India using digital shoreline analysis system. Spat. Inf. Res. 26, 563–571. https://doi.org/10.1007/s41324-018-0199-6
26. Shalowitz, A.L., 1964. Shore and sea boundaries: with special reference to the interpretation and use of Coast and Geodetic Survey data. US Department of Commerce.
27. Stafford, D.B., Langfelder, J., 1971. Air photo survey of coastal erosion. Photogramm. Eng. 37, 565–575.
28. Zhang, K., Huang, W., Douglas, B.C., Leatherman, S., 2002. Shoreline position variability and long-term trend analysis. Shore and Beach 70, 31–35.